Calculation of the cross sections for positron- and proton-impact ionization of helium

Zhifan Chen and A. Z. Msezane
Center for Theoretical Studies of Physical Systems and the Department of Physics, Clark Atlanta University, Atlanta, Georgia 30314
(Received 19 July 1993)

Cross sections for positron- and proton-impact ionization of atomic helium have been calculated using a coupled-state method. The single-electron Hamiltonian of the helium atom was diagonalized in a finite Hilbert space. We included nine radial pseudostates for each *s*, *p*, *d*, and *f* angular momentum. The time-dependent Schrödinger equation was solved by using a unitary matrix, *U* matrix, and a hyperbolic trajectory for both projectiles. Our positron results, covering the energy range 60–1000 eV, are compared with available measurements and theoretical calculations. Agreement with the most recent measurement is reasonably good over the entire positron energy range. The proton-impact cross sections are obtained for the proton energy range 10–1000 keV and also show good agreement with the measurements over the entire energy range. We conclude that the lower ionization cross sections for positron impact in comparison with those for proton impact are due to the bigger deflection suffered by the positron in the collision.

PACS number(s): 34.50.Fa, 34.10.+x, 31.50.+w

I. INTRODUCTION

Positron-helium scattering has continued to receive a great deal of attention, particularly in recent years [1–12]. Above the threshold of the helium, two ionization processes are possible. One is the impact ionization; the other is positronium formation. The ionization cross section of the helium atom by positron impact has been measured by Sueoka [1], Fornari, Diana, and Coleman [2], and Fromme *et al.* [3]. Recently, the cross section has also been obtained by Knudsen *et al.* [4] based on a time-of-flight measurement. The results of Knudsen *et al.* [4] and Fromme *et al.* [3] are almost the same when the positron energy is above 300 eV. However, they differ when the projectile energy is around 100 eV. Theoretically, positron-impact ionization is simpler to calculate than the electron-impact ionization because the exchange effects can be ignored.

The first quantum-mechanical calculation of the ionization cross section for positron impact of helium was carried out by Basu, Mazumdar, and Ghosh [9]. The initial positron was represented by a distorted-wave function. The final wave function was described by either the product of a plane wave and a Coulomb function or two unscreened Coulomb functions. The result of the product of a plane wave and a Coulomb function shows good agreement with the experimental data of Fromme *et al.* [3]. Campeanu, McEachran, and Stauffer [7] studied the detailed effect of the initial and the final states and the screening effect of the helium ion. Their calculations agree reasonably well with the data of Fromme *et al.* [3] in the positron energy range up to 300 eV. Schultz and Olson [8] used the classical trajectory Monte Carlo (CTMC) method to calculate the cross section for the same process. As expected, their data decrease too fast when the positron energy is above 200 eV. This is because the method does not include the resonant contribution to the ionization process.

Although the coupled-state method has been used to study the collision between the positron and the helium by Willis *et al.* [5], the main purpose of their calculation was to evaluate the excitation cross sections. The ionization cross section is then evaluated by using the measurements of the total cross sections by Blaauw *et al.* [6].

In this paper we have performed a pseudostate coupled-state calculation to evaluate the cross sections for positron- and proton-impact ionization of the helium atom. The calculations were carried out in the positron energy range from 60 to 1000 eV and the proton energy range from 10 to 1000 keV. The Hamiltonian of the helium atom was first diagonalized in a Hilbert discrete basis. The *U*-matrix method was then used to solve the coupled-state equation by propagating the wave function from $t=-\infty$ to $t=\infty$. The cross section for the ionization was obtained by summing over all the cross sections excited to the pseudostates whose energies are above the ionization threshold. The cross section for proton impact of helium has also been calculated and compared with the results of the positron.

II. THEORY

Coupled-state equations solved by a *U*-matrix approach have been used in previous calculations [13–17]. Even when the lighter particles, such as electrons, were used as the projectiles [13], good agreement has also been obtained in comparison with the experimental results in certain energy ranges. The use of this method is explained briefly below. The nucleus of the target is assumed to be stationary at the origin during the entire collision process. It is assumed that only one electron is ionized while the other electron is "frozen" during the collision. The problem is then reduced to a one-active-electron system. However, in reality, there are two electrons on the target; therefore a factor of 2 is introduced in the final cross sections to account for the two *K*-shell

electrons.

The single-electron Hamiltonian is first diagonalized in a finite Hilbert space with basis functions taken to be

$$\frac{Y_{lm}\pm Y_{lm}^{*}}{\sqrt{2}} r^{l} e^{-\alpha_j r}, \quad l\neq 0 \tag{1}$$

and

$$Y_{lm} r^{l} e^{-\alpha_j r}, \quad l=0, \tag{2}$$

where

$$\alpha_j = \frac{c_l}{a_n(1-\epsilon_l e^{-i\phi_j})}, \tag{3}$$

a_n is the Bohr radius for a hydrogenic atom of nuclear charge Z_n, ϕ_j are the angles taken equally spaced from 0 to 2π, Y_{lm} are the spherical harmonics, and c_l and ϵ_l are constants depending on the orbital angular momentum. This choice of basis allows a tremendous simplification in the calculation of the excitation matrix elements because each matrix element will have exactly the same form for different eigenfunctions. The Hartree-Fock bound states and discrete pseudostates which represent the continuum states will be obtained by diagonalization. In the calculation we have included nine radial pseudostates for s, p, d, and f angular momentum. Eight s states and all p, d, and f states are above the ionization threshold. They represent the ionization transition.

The wave function of the system satisfies the time-dependent Schrödinger equation. In the interaction picture it is given by

$$\left[i\hbar\frac{\partial}{\partial t} - V_I \right] \Psi_I(\mathbf{r},t) = 0, \tag{4}$$

where

$$V_I(t) = \exp\left[\frac{iH_0 t}{\hbar}\right] V \exp\left[-\frac{iH_0 t}{\hbar}\right], \tag{5}$$

H_0 is the Hamiltonian of the helium atom, and V is the interaction potential. The matrix elements of $V_I(t)$ were evaluated by introducing an expansion for V:

$$\frac{1}{|\mathbf{r}-\mathbf{R}|} = \sum_{L=l_1-l_2}^{L=l_1+l_2} \frac{4\pi}{2L+1} \sum_{M=-L}^{M=L} Y_{LM}(R) Y_{LM}(r) \times \left[\frac{r^L}{R^{L+1}}\theta(R-r) + \frac{R^L}{r^{L+1}}\theta(r-R) \right],$$

where R and r are the distances of the projectile and the target electron and l_1 and l_2 are the quantum numbers of the orbital angular momentum for states 1 and 2, respectively. At certain impact parameter b and time step t ($Z=vt$) the matrix elements of the $V_I(t)$ can be divided into two parts, the radial part and the angular part. The radial part can be calculated analytically, and it is only related to R ($R=\sqrt{b^2+Z^2}$). The angular part for each transition was performed by using the spherical harmonic functions. Five computational loops have been assigned for l_1, m_1, l_2, m_2, m_2, and L. They cover all the possible transitions. The details of the discussion can be found in Ref. [16].

The time development of the system may be represented by the action of a unitary operator, U matrix, which can propagate the system from time t_0 to time t,

$$\Psi_I(t) = U(t,t_0)\Psi_I(t_0). \tag{6}$$

Substituting Eq. (6) into Eq. (4) shows that the U-matrix $U(t,t_0)$ satisfies the differential equation

$$\left[i\hbar\frac{\partial}{\partial t} - V_I(t) \right] U(t,t_0) = 0. \tag{7}$$

Equation (7) can be written in the form

$$U(t,t_0) = I - \frac{i}{\hbar}\int_{t_0}^{t} V_I(t')U(t',t_0)dt', \tag{8}$$

where $I=U(t_0,t_0)$ is the identity matrix. Equation (8) can be iterated to solve for $U(t,t_0)$.

$$U(t,t_0) = I - \frac{i}{\hbar}\int_{t_0}^{t} V_I(t')dt' - \frac{1}{\hbar^2}\int_{t_0}^{t} dt' \int_{t_0}^{t'} dt'' V_I(t')V_I(t'') - \frac{i}{\hbar^3}\int_{t_0}^{t} dt' \int_{t_0}^{t'} dt'' \int_{t_0}^{t''} V_I(t')V_I(t'')V_I(t''')dt''' + \cdots. \tag{9}$$

Neglecting higher-order terms, Eq. (9) can be replaced by the approximation

$$U(t,t_0) \approx \exp\left[-\frac{i}{\hbar}\int_{t_0}^{t} V_I(t')dt'\right]. \tag{10}$$

Expression (10) is strictly true only if the $V_I(t')$ commutes with $\int_{t_0}^{t'} V_I(t'')dt''$ for every time step. This will be satisfactory if the time steps in the limit of the integral are small. The U matrix is now constructed as the product of the unitary matrices of the small time step. $V_I(t')$ can be written as $V_I(t')=f(t')\exp(iwt')$. $f(t')$ is slowly varying with time. The oscillation $\exp(iwt')$ becomes more severe when the energy difference between the initial and final states is big or time (t') is large. To handle this problem, a technique [17] was used to evaluate the integral. We fit the $f(t')$ with a parabola and calculate the rest of the integral exactly. This method greatly reduces the mesh of the integral. In the calculation, we divided the integral into 81 meshes, then reduced the mesh size by half to confirm the convergence.

The perturbation of the electronic states, provided by

$V_I(t)$, will lead to the transition from the initial state (i) to the final state (f). The probability amplitude P_{fi} of the transition $i \rightarrow f$, which is dependent on the projectile path, was obtained by squaring the U-matrix elements at time $t = \infty$,

$$P_{fi} = U_{f,i}(\infty, -\infty)^2 . \tag{11}$$

The cross section for the transition of $i \rightarrow f$ is given by

$$\sigma_{fi} = 2\pi \int_0^\infty P_{fi} b \, db , \tag{12}$$

where b is the impact parameter. The ionization cross section is the sum of all the cross sections that start from the 1s and end up in any of the continuum pseudostates. In the calculation we used a hyperbolic trajectory, which was determined by the deflecting force of the Coulomb repulsion between the projectile positron or proton and the target nuclei.

III. RESULTS

In Fig. 1 the cross sections for positron-impact ionization of helium are plotted against the positron energy. Also shown in the figure are the experimental data of Fromme *et al.* [3] and of Knudsen *et al.* [4] and the theoretical results of Campeanu, McEachran, and Stauffer [7] and Schultz and Olson [8]. The single-ionization cross section exhibits a maximum near 100 eV. There is a good agreement between our calculation and the experimental results of Knudsen *et al.* The calculation of Schultz and Olson around 100 eV also favor the data of Knudsen *et al.* When the positron energy is above 300 eV, our calculation agrees with the experimental data reasonably well. The calculations of Schultz and Olson [8] and of Campeanu, McEachran, and Stauffer [7] give no data of ionization cross sections in this energy range.

In Fig. 2 we display the results for proton-impact ionization of helium. Our ionization cross section shows very good agreement with the experimental data of Rudd *et al.* [10], Shah and Gilbody [11], Rudd and Madison [12], and Rudd, Sautter, and Bailey [18] in the energy range from 10 to 1000 keV. We note that in both Figs. 1 and 2, our results are slightly larger than the experimental data except around the cross-section maxima. This

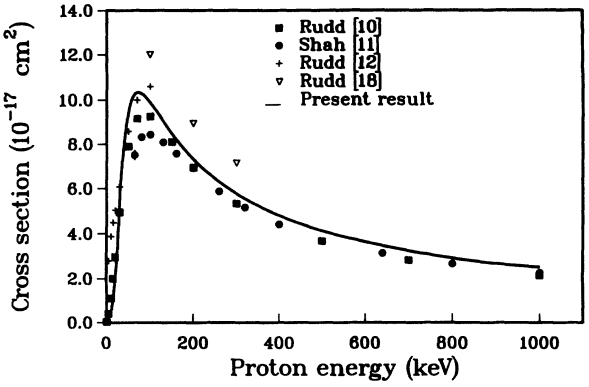

FIG. 2. Ionization cross sections of helium by proton impact.

may be caused by the fact that the ground state of the helium atom is represented approximately.

Our ionization cross section by proton and positron impact of helium are compared in Fig. 3 as a function of the collision velocity. The figure shows that the proton data is higher than that of the positron data. As the positron energy increases, the ionization cross section by positron impact approaches that by proton impact. In the calculation the only difference in the input parameters is the mass. Different masses cause different deflections of the projectiles. We can study the deflection effect by comparing the scattering angle at selected velocities, viz., $v = 3.09$ and 8.57 a.u. At $v = 3.09$ a.u. the ionization cross section by positron impact reaches a maximum. At $v = 8.57$ a.u. the ionization cross sections of the helium atom are almost the same by the proton and the positron impact.

Figure 4 shows the product of probability (p) and impact parameter (b) (in units of a_0, the first Bohr radius of the hydrogen atom) versus b for the collision velocity $v = 3.09$ a.u. The pb-vs-b curve shows a maximum at $b = 2a_0$. The scattering angles of the positron and the proton at this impact parameter are 22.3° and 1°, respectively. The larger deflection effect of the positron causes less interaction with the electron of the target and therefore the lower probability of ionization. When $b = 10a_0$ the scattering angle for the positron is reduced to 4.7°. The actual scattering angle will be smaller because we

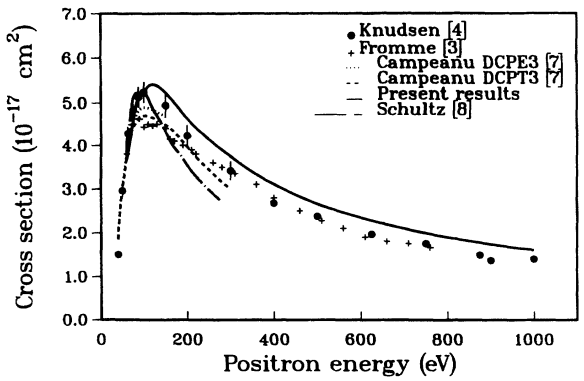

FIG. 1. Ionization cross sections for positron impact of helium.

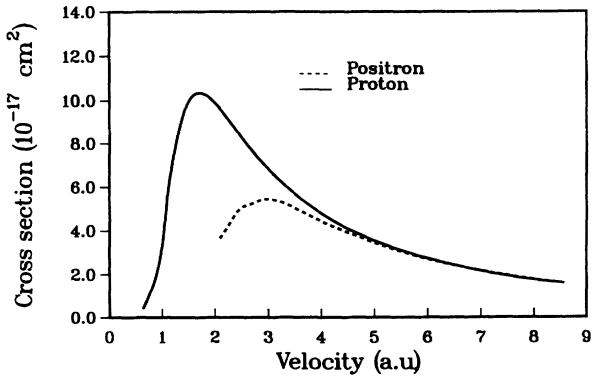

FIG. 3. Ionization cross sections of helium by proton and positron impact versus collision velocities.

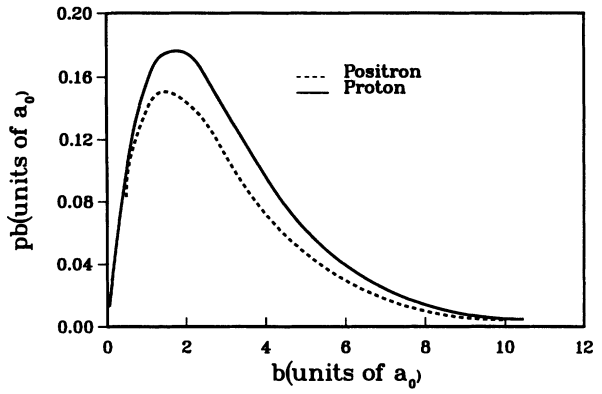

FIG. 4. Product of ionization probability and impact parameter versus b at the collision velocity of 3.09 a.u.

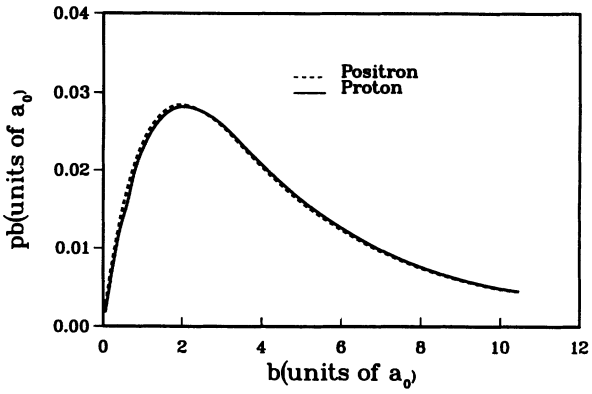

FIG. 5. Product of ionization probability and impact parameter versus b for proton and positron impact at the collision velocity of 8.57 a.u.

used the repulsive force of the target nucleus and the projectile to determine the path. This interaction should be screened by the electron. Therefore the scattering angle given here is the maximum angle for which the positron and the proton can have in the scattering. At large impact parameter, for example, $b=10a_0$, the scattering angle of the positron is small; therefore the interaction between the positron and the electron is similar to the interaction between the proton and the electron. The ionization probabilities of the proton and the positron approach the same values.

The pb-vs-b curve at $v=8.57$ a.u. is shown in Fig. 5. The figure indicates that the ionization probabilities of the proton and the positron are the same at any impact parameters. The curve has a maximum at $b=2.5a_0$. At this impact parameter the scattering angles of the positron and the proton are 2.4° and 0.0013°, respectively. The actual deflections are less than these angles, as stated above. Because the positron path is close to a straight line, the proton and the positron impact of helium have the same ionization probabilities. Our calculation and analysis show that as the mass of the proton is 1839 times heavier than that of the positron, the scattering angle for the positron is expected to be bigger than that of the proton. However, if the scattering angle is only a few degrees, the deflection will not greatly affect the ionization probability and hence the ionization cross section. When the scattering angle is larger than 20° the ionization cross section shows a difference from the result of the straight-line path of the projectile.

IV. CONCLUSION

A coupled-state method has been used to calculate the cross sections for positron- and proton-impact ionization of helium. The positron results are found to show good agreement with the most recent experimental data of Knudsen *et al.* in the entire energy range of 60–1000 eV. A comparison of the positron and the proton results at the same collision velocity indicates that the larger ionization cross section of the proton is caused by the smaller deflection suffered by the proton in the Coulomb repulsive potential.

ACKNOWLEDGMENTS

This work was supported in part by DOE, Office of Basic Energy Sciences, Division of Chemical Sciences and The National Science Foundation. The authors would like to thank Dr. Reading and Dr. Ford for their many helpful discussions.

[1] O. Sueoka, J. Phys. Soc. Jpn. **1**, 3757 (1982).
[2] L. S. Fornari, L. M. Diana, and P. G. Coleman, Phys. Rev. Lett. **51**, 2276 (1983).
[3] D. Fromme, G. Kruse, W. Raith, and G. Sinapius, Phys. Rev. Lett. **57**, 3031 (1986).
[4] H. Knudsen, L. Brun-Nielsen, M. Charlton, and M. R. Poulsen, J. Phys. B **23**, 3955 (1990).
[5] S. L. Willis, J. Hata, M. R. C. McDowell, C. J. Joachain, and F. W. Byron, Jr., J. Phys. B **14**, 2687 (1981); S. L. Willis and M. R. C. McDowell, *ibid.* **15**, L31 (1982).
[6] H. J. Blaauw, F. J. de Heer, R. W. Wagenaar, and D. Barends, J. Phys. B **10**, L299 (1977).
[7] R. I. Campeanu, R. P. McEachran, and A. D. Stauffer, J. Phys. B **20**, 1635 (1987).
[8] D. R. Schultz and R. E. Olson, Phys. Rev. A **38**, 1866 (1988).
[9] M. Basu, P. S. Mazumdar, and A. S. Ghosh, J. Phys. B **18**, 369 (1985).
[10] M. E. Rudd, Y. K. Kim, D. H. Madison, and J. W. Gallagher, Rev. Mod. Phys. **57**, 965 (1985).
[11] M. B. Shah and H. B. Gilbody, J. Phys. B **18**, 899 (1985).
[12] M. E. Rudd and D. H. Madison, Phys. Rev. A **14**, 128 (1976).
[13] M. H. Martir, A. L. Ford, J. F. Reading, and Becker, J.

Phys. B **15**, 1729 (1982).
[14] G. L. Swafford, J. F. Reading, A. L. Ford, and E. Fitchard, Phys. Rev. A **16**, 1329 (1977).
[15] Zhifan Chen and J. F. Reading, Phys. Rev. A **48**, 352 (1993).
[16] M. H. Martir, Ph.D. thesis, Texas A&M University, 1981 (unpublished).
[17] J. F. Reading, A. L. Ford, and E. Fitchard, Phys. Rev. Lett. **36**, 573 (1976).
[18] M. E. Rudd, C. A. Sautter, and C. L. Bailey, Phys. Rev. **151**, 20 (1966).